PHYSICAL REVIEW E **84**, 062701 (2011)

Conductivity anisotropy of assembled and oriented carbon nanotubes

Camilo Zamora-Ledezma,[1,3] Christophe Blanc,[2] Nicolas Puech,[1] Maryse Maugey,[1] Cécile Zakri,[1]
Eric Anglaret,[2] and Philippe Poulin[1]
[1]*Centre de Recherche Paul-Pascal, Université de Bordeaux–CNRS, 115 Avenue Schweitzer, F-33600 Pessac, France*
[2]*Laboratoire Charles Coulomb UMR 5221, Université Montpellier II, place Eugène Bataillon, F-34095 Montpellier Cedex 5, France*
[3]*Laboratorio de Física de la Materia Condensada, Centro de Física, Instituto Venezolano de Investigaciones Científicas,*
Altos de Pipe, 1204 Caracas, Venezuela

(Received 26 August 2011; published 28 December 2011; publisher error corrected 30 December 2011)

An assembly of packed and oriented rodlike particles exhibit anisotropic physical properties. We investigate in the present work the anisotropic conductivity of films made of intrinsically conducting rods. These films are obtained from more or less ordered carbon nanotube liquid crystals. Their orientational order parameter is measured by polarized Raman spectroscopy. A relationship between the anisotropy of surface conductivity and orientational order parameter is determined. The experimental results are accounted for by a model that takes into account the number of intertube contacts and density of conductive pathways in different directions, as introduced by J. Fischer *et al.* for magnetically aligned nanotubes. We find that a good agreement, without any fitting parameter, of the proposed model and experiments is obtained when we consider a two-dimensional (2D) Gaussian distribution of the nanotube orientation. The conductivities parallel and perpendicular to the nematic director differ by almost an order of magnitude. This anisotropy is much greater than that of conventional dielectric liquid crystals, where the behavior is governed by the mobility anisotropy of ionic current carriers. The present results do not depend on the intrinsic properties of the nanotubes and are expected to be relevant for other assemblies of conducting rodlike particles, such as metallic or semi-conducting nanowires and ribbons.

DOI: 10.1103/PhysRevE.84.062701 PACS number(s): 61.30.−v, 73.61.Ph, 81.07.−b, 82.70.−y

Introduction. Conducting and anisometric particles, such as carbon nanotubes (CNTs) and metallic or semi-conducting nanowires and ribbons, are potentially useful to achieve conductive films that find applications in electronic components, capacitors, sensors, electromechanical actuators, etc. CNTs are promising materials in this field because of their high aspect ratio and chemical stability. Packing and aligning CNTs on a large scale is a route towards the optimized manifestation of their intrinsic axial properties in a macroscopic film. Various methods have been proposed over recent years to achieve packed assemblies of aligned CNTs. These methods include composite drawing [1–4], application of external fields [5–8], flow induced alignment [9–11], and liquid crystal templating and ordering [12–30]. The latter approach is particularly appealing because it is based on the thermodynamical properties of the material at equilibrium. Liquid crystals exhibit anisotropic physical properties such as optical birefringence and anisotropic dielectric constants [31]. They also exhibit conductivity anisotropy. In dielectric liquid crystals, the current carrying species are generally embedded ions. The conductivity anisotropy results from the differences of the ionic mobility parallel and perpendicular to the director field [31]. This phenomenon has been the topic of several studies in the past. In contrast, the current is carried by electrons traveling through the particles in a film made from a liquid crystal of intrinsically conductive particles. While conductivity anisotropy has been experimentally observed in a number of aligned CNT materials, a quantitative relationship between the conductivity anisotropy and the degree of ordering has yet to be determined. This relationship is expected to be relevant for a variety of materials from rigid conducting polymers to metal nanowires and carbon nanotubes. We report in the present work an experimental determination of this relationship. Different films made from more or less ordered liquid crystals are prepared. The order parameters of the systems are measured by polarized Raman spectroscopy [4,28,29,32]. It is observed that the conductivity anisotropy strongly increases with the order parameter. The experimental results are in good agreement with a statistical model that takes into account the number of intertube contacts and conductive paths [6] when a two-dimensional (2D) Gaussian distribution of the nanotube orientations is considered. The involved conductivity mechanisms can lead to typical ratios of conductivity parallel and perpendicular to the nematic director up to 8 for an order parameter of about 0.6. This degree of anisotropy is much greater than the conductivity anisotropy of liquid crystals resultant from the mobility anisotropy of embedded ions. Indeed, anisotropy conductivity arising from differences in ionic mobility does not generally exceed a value of 2 in dielectric liquid crystals [31].

Results and discussions. The present liquid crystals are made of surfactant stabilized aqueous suspensions of carbon nanotubes. Already published approaches are followed to achieve nematic liquid crystals with different order parameters [29]. The degree of ordering is controlled by the dispersion process as described below. Single walled Elicarb® carbon nanotubes from Thomas Swan (UK) (batch number K3772) are presently used. Bile salts (BS) which are mixtures of cholic acid and deoxycholic acid sodium salts were purchased from Fluka and used as dispersants. The CNT suspensions are homogenized by sonication with a Branson Sonifier S-250A equipped with a 3-mm tapered microtip and operating at 20 kHz. The sonication time was varied in order to shorten the nanotubes [33,34] and improve their dispersion. The sonicator power was set at 20 W and delivered by pulses of 0.5 s separated by 0.2 s intervals at rest. The samples are kept in an ice bath during sonication in order to avoid overheating. All starting suspensions contain 0.5 wt% CNT and 0.5 wt% BS in water. They are in an isotropic state in these conditions. Ultracentrifugation is used to increase the CNT concentration and achieve nematic liquid crystals. It was recently shown that short and straight CNTs align more easily than long and wavy CNTs, which often exhibit kinks and structural defects. CNT shortening is achieved by high-power sonication [29]. Sorting by ultracentrifugation [29,35,36] allows improvements of the nematic order parameter via the selection of the shortest and straightest nanotubes. Two sets of samples are made at two different sonication times $T_{\mathrm{US}} = 30$ and 180 min. Each suspension is then ultracentrifugated in three subsequent steps: (i) 45 min at $2000g$, (ii) 45 min at $2\,10\,000g$ and (iii) 180 min at $2\,10\,000g$. After each ultracentrifugation, the supernatant is carefully removed and kept for the following centrifugation step. The bottom concentrated part is found to be in a nematic state. This sediment fraction is collected into a separated vial at each ultracentrifugation step. Samples will be called first, second, and third nematics for sediments respectively collected after the first, second, and third centrifugation. Tip sonication is known to be efficient at unbundling nanotubes [33]. Nevertheless, a complete unbundling is not achieved even for the longest sonication time, and the first sediment presumably contains a non-negligible fraction of nanotube bundles. But the presence of bundles does not affect the characterization of the materials and the measurements of the order parameter via the present analyses. We also note that the exact length of the presently used materials is not known. Nevertheless, considering studies of similar materials dispersed via tip sonication in surfactant solutions [29,33], the average length of the shortest nanotubes is expected to be on the order of a few hundred nanometers. Dry and conductive films are made with each nematic liquid crystal. For this, a drop of liquid crystal is deposited onto a glass slide and sheared with a second glass slide on top of it. Uniaxial monodomains of macroscopic areas of about 2×3 cm^2 are obtained thereby [28]. The upper slide is removed so that the films can dry to form ordered assemblies of packed CNTs. The thickness of the films is about 100–150 nm, as measured with a mechanical profilometer and by atomic force microscopy.

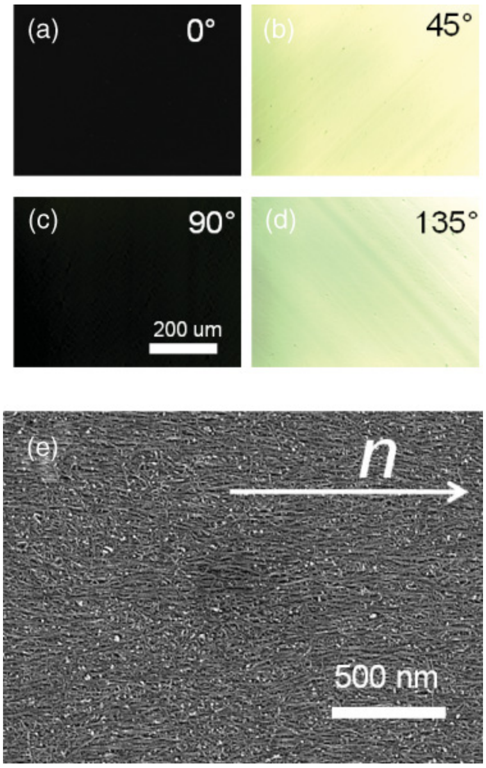

FIG. 1. (Color online) (a)–(d) Optical micrographs between crossed polarizers in horizontal and vertical directions of a CNT thin film rotated at various angles with respect to the polarizer axes. The angles are indicated on each micrograph. The sample has been sheared along the horizontal direction. The observed differences in transmitted light reveal the alignment of the carbon nanotubes along the shear direction. (e) High-resolution scanning electron micrograph of the same film. The nematic director is specified by the arrow.

Typical optical micrographs in transmission mode and between crossed polarizers of an anisotropic CNT film are shown in Fig. 1. The transmitted light strongly depends on the relative orientation of the shear direction to the polarizers' axes. This observation qualitatively confirms that CNT ordering is maintained during drying. The CNT orientation is revealed at a microscopic level by high-resolution scanning electron microscopy as shown in Fig. 1(e). The CNTs are, as expected, well oriented along the shear direction and seem to lie in the plane of the film. The CNT concentration in the nematic phase is typically a few wt%. Considering for example a reasonable value of 5 wt%, the weight fraction of solid content is expected to be multiplied by a factor of 20 during drying. Water evaporation results therefore in a strong decrease of the film thickness and in the quasi-2D confinement of the nanotubes. The sheared and dried films are thinner than the average nanotube length. Considering the present confinement conditions, it is assumed that the contribution of nanotubes pointing out of the plane can be neglected in the estimation of the order parameter. The degree of ordering was quantitatively characterized using polarized spectroscopy [28]. The average orientation of the nematic is specified by a unit vector called the nematic director. In two dimensions, the scalar order parameter is given by

$$S = \langle 2\cos^2\theta - 1\rangle, \qquad (1)$$

where θ is the angle that a CNT makes with the nematic director. S is deduced from Raman measurements carried out using a laser line at 1064 nm (1.16 eV) of a Nd:YAG laser and a Fourier transform Bruker RFS100 spectrometer. Spectra are measured in three different polarization configurations: VV, VH, and HH, where V or H correspond to polarizations of the incident and scattered waves parallel or perpendicular to the alignment direction. Typical polarized Raman spectra are shown in Fig. 2. The main typical bands RBM, D, G, and G′ are labeled. Corrections for dichroism are taken into account in the determination of S [4,28]. The strong differences of scattered intensity as a function of the configuration reflect the ordering of the CNTs. As expected [29], the degree of ordering increases substantially from about $S \sim 0.1$ for the first nematics up to almost $S \sim 0.6$ for the third nematics. However, little difference was observed between CNTs sonicated for 30 min and CNTs sonicated for 180 min. A 5×5 mm^2 square is isolated on each film. Edges parallel and perpendicular to the shear direction

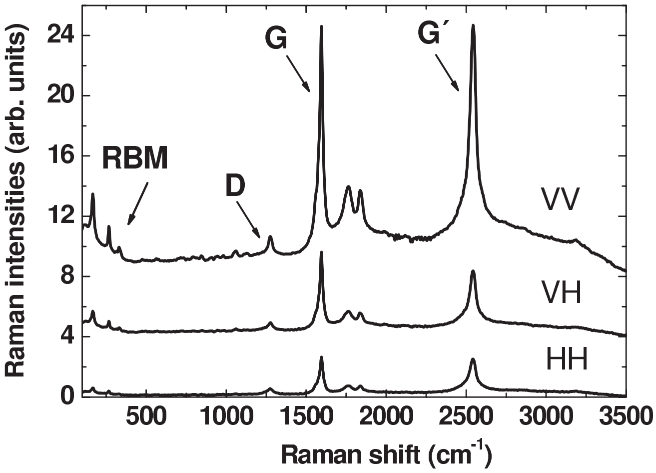

FIG. 2. Polarized Raman spectra of an anisotropic nematic film prepared from the third nematic nanotube based liquid crystals defined in the text. The films are excited with an incident laser beam at 1064 nm. The spectra are shifted along the ordinate axis for clarity. The main bands (RBM, D, G and G′) are labeled.

are subsequently coated with silver paste. As sketched in Fig. 3(a), the silver coatings serve as electrodes for surface conductivity measurements. The latter are carried out at room temperature using a Keithley 2000 multimeter. We note that four-probe measurements have been tested and gave results similar to those obtained by two-probe measurements. This reflects that the electrode contact resistances are negligible compared to the resistance of the CNT films. The samples are kept at 80 °C under vacuum for 24 h prior to each measurement in order to avoid artifacts due to the presence of moisture. The conductivity of the present nanotube assemblies is limited by the resistivity of the intertube contacts. Net values of the surface resistivity typically range from 10^3 to 10^4 Ω/square for the investigated samples. These values depend on the nanotube features, including length, aspect ratio, electronic properties, and presence of remaining surfactant molecules at the CNT interfaces. In particular, surfactants at the nanotube interfaces are expected to increase the contact resistance between neighboring nanotubes. By contrast, the surface conductivity anisotropy defined by the ratio between the surface conductivity parallel to the nematic director and the perpendicular one, $\sigma_{\text{ani}} = \sigma_{\parallel}/\sigma_{\perp}$, does not depend on such features. This ratio is expected to depend only on the ordering and anisotropy of the nanotube assembly. It is actually observed that σ_{ani} increases with the order parameter. σ_{ani} is close to 1 for films that are weakly ordered. It increases up to $\sigma_{\text{ani}} \sim 8$ for the more ordered third nematics with an order parameter $S \sim 0.6$.

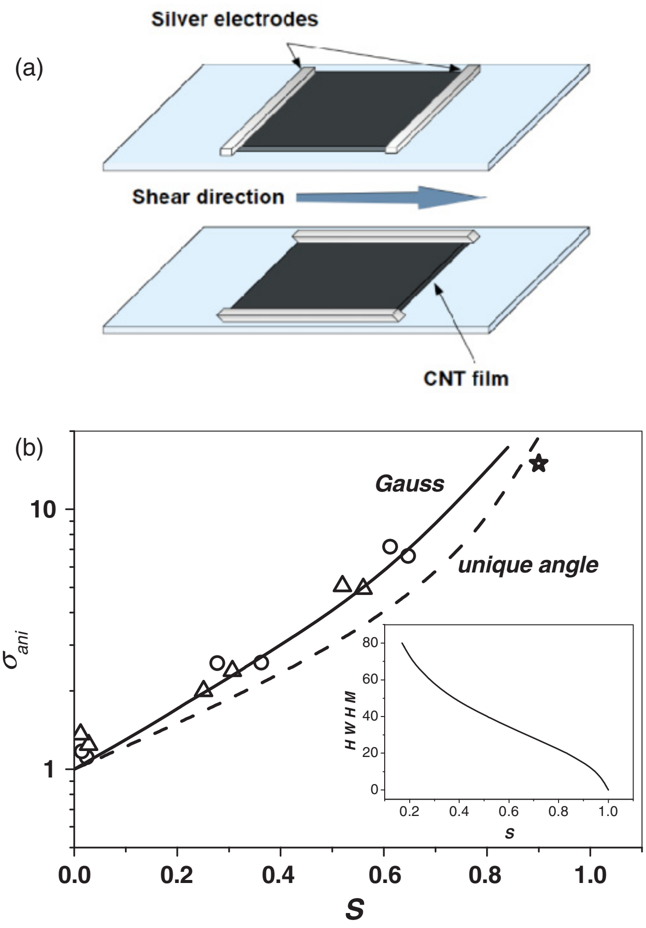

FIG. 3. (Color online) (a) Scheme of the setup for conductivity measurements. (b) Surface conductivity anisotropy as a function of the order parameter. Circles and triangles respectively correspond to samples sonicated for 30 and 180 minutes. The star corresponds to the anisotropy conductivity of materials investigated by Lu and Chen [14]. The dashed curve corresponds to the conductivity anisotropy calculated in equation [2] considering a single value for the θ angle. The continuous curve corresponds to the anisotropy calculated for an ordered assembly of conducting rods without any fitting parameter and with a 2D Gaussian distribution of their orientation with respect to the nematic director. The approximate half-width at half maximum (HWHM) of the orientation distribution as a function of S is given in the inset. This value is here given in degrees.

The present experimental results allow a quantitative discussion on the mechanisms responsible for the observed conductivity anisotropy. J. Fischer *et al.* modeled magnetically aligned CNT films as an ensemble of 1D conducting paths in the plane of the sample [6]. Each path contains on average n particles of fixed length. Consequently the resistance of each path is proportional to n (conductance proportional to $1/n$). This model considers that the electrical current is limited by the intrinsic resistivity of the nanotubes. Intertube contacts are in fact the most resistive components and have to be taken as the limiting species to estimate the conductivity. But evaluating the number of intertube contacts and evaluating the number of nanotubes are equivalent as long as 1D paths are considered. This is why the model proposed by Fischer *et al.* can still be used for the estimation of the surface conductivity anisotropy of the presently investigated materials. For a given total number of particles N, the number of paths is N/n. Assuming that the conducting paths are in parallel in a given direction, the conductance of the ensemble is directly proportional to N/n times $1/n$, the conductance of a path along the considered direction. The resistance is therefore expected to scale as n^2. The average number of particles required to connect edges of the film differs along the vertical and horizontal directions because of the CNT alignment. This average number is proportional to the projection length of the nanotubes on the considered axes of the film. The resultant conductivity anisotropy is therefore expected to be

$$\sigma_{\mathrm{ani-cal}} = \left[\frac{\langle \cos\theta \rangle}{\langle |\sin\theta| \rangle} \right]^2 . \tag{2}$$

Unfortunately this relationship could not be tested as a function of S by Fischer *et al.* because the anisotropy predicted from Raman scattering measurements was almost similar for the two samples investigated by the authors [6]. More recently, Lu and Chen achieved a macroscopically aligned conductive film from a CNT liquid crystal [14]. The authors estimated from electron micrographs an order parameter of about 0.9 for this film. The surface conductivity anisotropy is about 18. Unfortunately this single value does not yet allow a full comparison with the proposed model since it is obtained for a single system. In addition, determination of the order parameter at the surface of the film may differ from the order parameter of the bulk through which electrical current circulates. Taking advantage of the present Raman spectroscopy characterizations and of the possibility to vary the order parameter of the films, a first quantitative analysis of the conductivity anisotropy is here reported. Estimation of the surface conductivity in equation [2] necessitates the definition of a distribution for the θ angle. For example, the relationship represented by the dashed line in Fig. 3(b) is obtained by assuming that θ has a single fixed value to yield a given order parameter. The corresponding surface conductivity anisotropy is calculated according to equation [2] and plotted as a function of S. Even though such a bimodal distribution is poorly realistic, it is not far from yielding the anisotropy conductivity observed by Lu and Chen. However, it cannot account for the presently obtained results. Other forms of distributions, presumably more realistic, have to be tested. For this, we assume that the carbon nanotubes lie in the plane of the substrate and are distributed in two dimensions with a Gaussian distribution of their orientation:

$$p(\theta) = \frac{a}{\sqrt{2\pi\sigma^2}} e^{-\frac{\theta^2}{2\sigma^2}}, \quad \text{with} \quad \int_{-\pi/2}^{\pi/2} p(\theta) d\theta = 1.$$

Such a distribution could result for example from the thermal equilibrium of the confined nanotubes during drying. Indeed, the lowest-order term of the energy penalty of a nanotube deviating from the main alignment direction is expected to scale as θ^2. The resultant Boltzmann distribution of nanotube orientations will therefore adopt the Gaussian form given above. The variance σ and normalization factor a of $p(\theta)$ are chosen in order to yield defined order parameters. The value $\sqrt{2\ln(2)}\sigma$ provides an approximate value of the half-width at half maximum (HWHM) of the distribution comprised between $-\pi/2$ and $\pi/2$. This value is plotted as a function of S in the inset of Fig. 3(b). Averaging the number of conducting paths along different directions in equation [2] can then be done using the Gaussian distributions associated with different order parameters. This allows the surface conductivity anisotropy to be computed as a function of S without any fitting parameter. The results shown in Fig. 3(b) reveal a good agreement of the computed and experimental data. This good agreement strongly supports that the present approach captures the main involved physical mechanisms.

Conclusion. An experimental relationship between the order parameter and conductivity anisotropy of packed and ordered conducting rods has been reported. The achieved results show that the conductivity anisotropy is dominated by the distributions of conducting paths throughout the material along different directions. In contrast to dielectric liquid crystals, the presently involved mechanisms can lead to very large values of conductivity anisotropy. The present results do not depend on the intrinsic properties of the nanotubes and should be relevant for other assemblies of conducting rodlike particles, such as metallic or semiconducting nanowires and ribbons. We thus hope that this work can be helpful for the design and optimization of functional and widespread electromaterials made of assembled and ordered conducting anisotropic particles.

Acknowledgments. We thank the European Commission and the ANR for financial support of this work in the frame of the COMPLOIDS and NATALI projects. We thank Dr. Carlos Drummond for Atomic Force Microscopy (AFM) measurements and helpful discussions.

[1] R. Haggenmueller, H. H. Gommans, A. G. Rinzler, J. E. Fischer, and K. I. Winey, Chem. Phys. Lett. **330**, 219 (2000).

[2] P. Miaudet, S. Badaire, M. Maugey, A. Derre, V. Pichot, P. Launois, P. Poulin, and C. Zakri, Nano Lett. **5**, 2212 (2005).

[3] P. Potschke, H. Brunig, A. Janke, D. Fischer, and D. Jehnichen, Polymer **46**, 10355 (2005).

[4] C. Zamora-Ledezma, C. Blanc, and E. Anglaret, Phys. Rev. B **80**, 113407 (2009).

[5] Z. Chen, Y. Yang, Z. Wu, G. Luo, L. Xie, Z. Liu, S. Ma, and W. Guo, J. Phys. Chem. B **109**, 5473 (2005).

[6] J. E. Fischer, W. Zhou, J. Vavro, M. C. Llaguno, C. Guthy, R. Haggenmueller, M. J. Casavant, D. E. Walters, and R. E. Smalley, J. Appl. Phys. **93**, 2157 (2003).

[7] B. W. Smith, Z. Benes, D. E. Luzzi, J. E. Fischer, D. A. Walters, M. J. Casavant, J. Schmidt, and R. E. Smalley, Appl. Phys. Lett. **77**, 663 (2000).

[8] K. Kordas, T. Mustonen, G. Toth, J. Vahakangas, A. Uusimaki, H. Jantunen, A. Gupta, K. V. Rao, R. Vajtai, and P. M. Ajayan, Chem. Mater. **19**, 787 (2007).

[9] S. B. Kharchenko, J. F. Douglas, J. Obrzut, E. A. Grulke, and K. B. Migler, Nature Mater. **3**, 564 (2004).

[10] B. Vigolo, A. Penicaud, C. Coulon, C. Sauder, R. Pailler, C. Journet, P. Bernier, and P. Poulin, Science **290**, 1331 (2000).

[11] S. Abbasi, P. J. Carreau, and A. Derdouri, Polymer **51**, 922 (2010).

[12] L. Dai, A. Patil, X. Gong, Z. Guo, L. Liu, Y. Liu, and D. Zhu, ChemPhysChem **4**, 1150 (2003).

[13] S. Zhang and S. Kumar, Small **4**, 1270 (2008).

[14] L. Lu and W. Chen, ACS Nano **4**, 1042 (2010).

[15] G. Scalia, ChemPhysChem **11**, 333 (2010).

[16] M. D. Lynch and D. L. Patrick, Nano Lett. **2**, 1197 (2002).

[17] V. Weiss, R. Thiruvengadathan, and O. Regev, Langmuir **22**, 854 (2006).

[18] P. van der Schoot, V. Popa-Nita, and S. Kralj, J. Phys. Chem. B **112**, 4512 (2008).

[19] J. P. F. Lagerwall and G. Scalia, J. Mater. Chem. **18**, 2890 (2008).

[20] J. Lagerwall, G. Scalia, M. Haluska, Dettlaff-U. Weglikowska, S. Roth, and F. Giesselmann, Adv. Mater. **19**, 359 (2007).

[21] I. Dierking, G. Scalia, and P. Morales, J. Appl. Phys. **97**, 044309 (2005).

[22] W. H. Song, I. A. Kinloch, and A. H. Windle, Science **302**, 1363 (2003).

[23] C. Zakri and P. Poulin, J. Mater. Chem. **16**, 4095 (2006).

[24] S. Badaire, C. Zakri, M. Maugey, A. Derre, J. N. Barisci, G. Wallace, and P. Poulin, Adv. Mater. **17**, 1673 (2005).

[25] M. F. Islam, A. M. Alsayed, Z. Dogic, J. Zhang, T. C. Lubensky, and A. G. Yodh, Phys. Rev. Lett. **92**, 088303 (2004).

[26] S. E. Moulton, M. Maugey, P. Poulin, and G. G. Wallace, J. Am. Chem. Soc. **129**, 9452 (2007).

[27] P. K. Rai, R. A. Pinnick, A. N. G. Parra-Vasquez, V. A. Davis, H. K. Schmidt, R. H. Hauge, R. E. Smalley, and M. Pasquali, J. Am. Chem. Soc. **128**, 591 (2006).

[28] C. Zamora-Ledezma, C. Blanc, M. Maugey, C. Zakri, P. Poulin, and E. Anglaret, Nano Lett. **8**, 4103 (2008).

[29] N. Puech, C. Blanc, E. Grelet, C. Zamora-Ledezma, M. Maugey, C. Zakri, E. Anglaret, and P. Poulin, J. Phys. Chem. C **115**, 3272 (2011).

[30] N. Puech, E. Grelet, P. Poulin, C. Blanc, and P. van der Schoot, Phys. Rev. E **82**, 020702 (2010).

[31] L. M. Blinov, *Electro-optical and Magneto-optical Properties of Liquid Crystals* (Wiley, New York, 1983).

[32] E. Anglaret, A. Righi, J. L. Sauvajol, P. Bernier, B. Vigolo, and P. Poulin, Phys. Rev. B **65**, 165426 (2002).

[33] S. Badaire, P. Poulin, M. Maugey, and C. Zakri, Langmuir **20**, 10367 (2004).

[34] A. Lucas, C. Zakri, M. Maugey, M. Pasquali, P. van der Schoot, and P. Poulin, J. Phys. Chem. C **113**, 20599 (2009).

[35] J. A. Fagan *et al.*, Adv. Mater. **23**, 338 (2011).

[36] M. S. Arnold, A. A. Green, J. F. Hulvat, S. I. Stupp, and M. C. Hersam, Nature Nanotech. **1**, 60 (2006).